Available online at www.sciencedirect.com

ScienceDirect

Proceedings of the Combustion Institute 37 (2019) 3767–3774

Proceedings of the Combustion Institute

www.elsevier.com/locate/proci

Flame spread and burning rates through vertical arrays of wooden dowels

Lin Jiang [a], Zhao Zhao [b], Wei Tang [b], Colin Miller [b], Jin-Hua Sun [a], Michael J. Gollner [b,*]

[a] *State Key Laboratory of Fire Science, University of Science and Technology of China, Hefei 230026, Anhui, China*
[b] *Department of Fire Protection Engineering, University of Maryland, College Park, MD 20742, USA*

Received 30 November 2017; accepted 4 September 2018
Available online 20 September 2018

Abstract

Fuel loads in real-world fire scenarios often feature discrete elements, discontinuities, or inhomogeneities; however, most models for flame spread only assume a continuous, homogeneous fuel. Because discrete fuels represent a realistic scenario not yet well-modeled, it is of interest to find simple methods to model fire growth first in simple, laboratory-scale configurations. A detailed experimental and theoretical study was therefore performed to investigate the controlling mechanisms of flame spread through arrays of wooden dowels, with dowel spacings of 0.75, 0.875, and 1.5 cm. Flames were found to spread vertically for all spacings; however, for the 1.5 cm spacing, the gap was too large for horizontal flame spread to occur. A radiation-controlled model for horizontal flame spread was developed that predicted the horizontal flame spread rate through various arrays of dowels. Combined with an existing convection-based model for vertical flame spread, both horizontal and vertical flame spread was modeled to predict the number of burning wooden dowels as a function of time. Using models for the burning rate of wooden dowels and boundary-layer theory, a global burning rate model was developed that provided reasonable agreement with experimental results.

Keywords: Flame spread; Wooden dowel; Heat transfer; Mass loss rate

1. Introduction

Predictions of both flame spread rates and the burning behavior of materials have long been goals for fire safety researchers. The majority of existing models for flame spread assumes that fuels are a continuous surface [1–5] or approximate them as a homogeneous porous medium [6]. In many real fires, however, flames spread between discrete fuel elements with properties that cannot be assumed to be homogeneous. While these scenarios can sometimes be modeled with complex multi-physics simulations [7,8], there is often a need to apply simple models for prediction of overall flame spread and burning rates during fire safety design.

Arrays of wooden sticks have provided useful surrogates to model discrete flame spread phenomena. Most of these experiments were performed

* Corresponding author.
E-mail address: mgollner@umd.edu (M.J. Gollner).

https://doi.org/10.1016/j.proci.2018.09.008
1540-7489

horizontally in quiescent flow [9,10] or in wind-driven scenarios [11–13], which closely modeled a wildfire configuration. In horizontal flame spread, the flame spread direction is perpendicular to the flow of buoyant gases, and, without wind, a steady state of spread is reached because the radiation received by neighboring wooden dowels is steady and determined by the dowel spacing [9]. Unlike flame spread over horizontal wooden arrays, where a steady state exists, vertical flame spread is driven by convection resulting in an accelerating process after ignition [10]. The goal of this paper is to further explore the mechanisms of both horizontal and vertical flame spread through arrays of wooden dowels and apply simple models to capture the 2-D flame progression. This is then expanded upon with a boundary-layer convection theory to predict the mass-loss rate over full arrays of wooden dowels. The results of this study represent a step towards understanding and modeling flame spread over discrete combustibles and provide a framework for future, larger-scale studies.

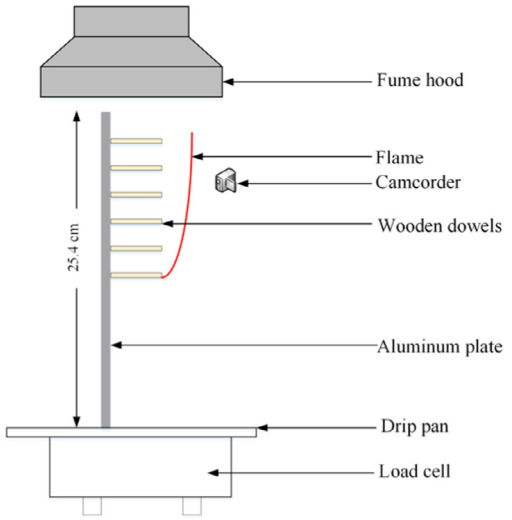

Fig. 1. Diagram of experimental apparatus for flame spread over wooden dowel arrays with $n = 6$ vertical rows, shown from a side view.

2. Literature review

Most work investigating flame spread through discrete fuels has been performed using wooden sticks of various sizes where the flame spreads in either horizontal or sloped configuration. Vogel and Williams [9] used vertical wooden matchsticks to model horizontal discrete fuel flame propagation by changing the length and spacing of matchsticks and determining necessary conditions for discrete fuel flame spread. Using a constant flame temperature and stand-off distance, a convection-controlled theory was developed which had good agreement with experimental results. Emmons and Shen [14] investigated flame spread over arrays of horizontal paper strips standing on their edges, where after an initial transient phase there existed two modes of steady burning. Steady flame spread rates were correlated with high and low values of a spacing ratio, but not for intermediate ones. Prahl and Tien [15] investigated horizontal flame spread over vertically-oriented matchsticks and paper strips by adding an opposed wind velocity. By considering fundamental theory, correlations between flame spread, wind velocity, fuel spacing, and fuel height were explored. Wolff et al. [12,13] investigated wind-aided flame spread over arrays of discrete fuel elements and found that the flame spread rate is proportional to $(U/m)^{1/2}$ over a wide range of wind speed, U, and fuel-mass distribution, m. Recently, Gollner et al. [10] investigated flame spread through a single vertical column of matchsticks. Based on the observed phenomenon, buoyancy was expected to control flame spread between matchsticks, and a theory based on convective heat transfer was developed to predict flame spread and burning rates.

3. Experimental setup

Wooden birch dowels were chosen for this study with a diameter of 0.32 cm cut to a sample length of 3.18 cm. This sample length was selected because it was long enough to avoid pure wall burning and associated boundary-layer effects, but also short enough to avoid warping of the dowels during the flame spread process. At this small diameter, a thermally-thin assumption is reasonable because the diameter of the dowel is much less than its thermal penetration depth, $\delta_T \approx k_s(T_p - T_\infty)/\dot{q}'' \approx 4.86$ mm, where k_s and T_p are the thermal conductivity and pyrolysis temperature of the dowel, respectively, T_∞ is the ambient temperature and $\dot{q}''$ is the heat flux from the flame to the unignited dowels [10]. Properties of the dowel are evaluated at ambient conditions (see Table 1) while the heat flux is estimated from the model presented in Section 5.

Figure 1 shows the experimental setup from which the flame spread behavior and the global mass loss can be captured simultaneously. Three aluminum plates painted with temperature-resistant matte black paint and with pre-drilled holes separated at 1.5, 0.875, and 0.75 cm were used to support the wooden dowels, leaving 2.68 cm exposed. An AND GF-6100 load cell was used to measure mass loss with an accuracy of 0.01 g at 2 Hz. To begin, a standard butane lighter was used to ignite one dowel placed below the center of the square arrays. A metal plate was held above this dowel when first ignited to avoid preheating in the array. To observe flame spread through and ignition of wooden dowels, a high-speed CASIO

Table 1
Properties used in horizontal and vertical flame spread calculations.

	Property	Quantity	Citation
ρ_s	Density of wood	500 kg m^{-3}	[23]
$c_{p,s}$	Specific heat of wood	2400 J kg^{-1} K^{-1}	[23]
ρ_g	Density of air	1.205 kg m^{-3}	[24]
$c_{p,g}$	Specific heat of air	1000 J kg^{-1} K^{-1}	[24]
B	Mass-transfer number	1.75	[10, 25]
d	Wooden dowel diameter	3.2×10^{-3} m	
k_s	Solid conductivity	0.15 W m^{-1} K^{-1}	[24]
l	Wooden dowel length	3.18×10^{-2} m	
T_f	Flame temperature	2270 K	[10]
T_p	Pyrolysis temperature	650 K	[10, 23]
T_0	Ambient temperature	298 K	

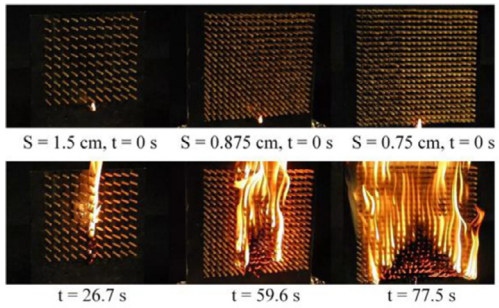

Fig. 2. Flame spread over wooden dowel arrays with different spacings, 1.5, 0.875, and 0.75 cm.

EX-F1 camcorder was used at an angle slightly off the center line of the wooden dowel array (see Fig. 2). Ignition was distinguished when at least 50% of the dowel surface was observed to be blackened. When recording video at 300 fps, the surface of individual dowels was observed, on average, every 5 frames due to swaying of the flame, giving an accuracy of 1/60 of a second, more than adequate for the slow rate of flame spread observed.

To verify the radiation-controlled model developed for horizontal flame spread, horizontal spread experiments with different spacings and row numbers ranging from 3 to 8 were performed. Experiments were ignited from the bottom of the leftmost column with a metal plate held between the first and second columns during ignition to avoid flame preheating, similar to vertical experiments. For the 1.5 cm spacing, the gap was too large to ignite adjacent dowels and support horizontal flame spread. For the 0.875 and 0.75 cm spacings, experiments with 1 and 2 rows did not produce a large enough flame to ignite adjacent dowels and support horizontal flame spread, hence they are not included here. Flame heights were determined by manually selecting the tallest extent of the visible flame taken from front-view video of horizontal flame spread. All experiments were repeated at least 2–3 times to ensure repeatability and assess errors.

4. General observations

After removal of the steel plate, the flame extends above the first dowel and begins to impinge upon and heat the second-row dowel. Additional layers above the second row can also receive heating before ignition due to natural convection from hot gases, which greatly accelerates the process of flame spread. For the dowels horizontally adjacent to the ignited dowel, the heat transfer is much lower than that received in the vertical direction, assumed to occur primarily due to flame radiation. After ignition, the flame will spread along the vertical direction first and, after the radiation from the growing flame to the unignited dowels to the side is large enough, a neighboring virgin dowel will ignite in the horizontal direction. As the duration of burning can be predicted by a burnout time, ignition via a convection-based theory, and horizontal spread via a radiation-based theory, these can be coupled into a two-dimensional model of flame spread through an array.

In this study, we performed flame spread experiments for three different spacings, 0.75, 0.875, and 1.5 cm, as shown in Fig. 2. For the 1.5 cm spaced array, the flame only spread along the center column of the array, similar to previous experiments [10]. The large spacing creates a situation in which the flames cannot ignite any horizontal dowels before the dowels ignited along the centerline burn out. This could also be calculated quantitatively through the burn-out time of burning dowels, t_b, and the ignition time of a virgin dowel due to horizontal radiative heating, t_i. For a 1.5 cm spaced array, using Eqs. (1,6–8), t_b is calculated to be smaller than t_i ($t_b = 13.6\,\text{s} < t_i = 19.8\,\text{s}$), which means that flames burn out before spreading horizontally, resulting in only a single column burning upwards.

For $S = 0.75$ and 0.875 cm arrays, adjacent dowels receive more radiation from the flame due to their smaller horizontal spacing. After removal of

the steel plate, the flame begins to spread rapidly along the vertical direction, dominated by natural convection, while the slower radiation-driven flame spread process allows the flames to spread horizontally throughout the array. Due to the difference in vertical to horizontal spread rates, the burning front eventually resembles a V-shaped pattern, reaching the top of the array far before reaching the sides, and leaving the sides of some horizontal rows untouched near the base of the array. For the smallest spacing, $S = 0.75$ cm, flames quickly spread vertically and horizontally, still forming a V pattern but not as pronounced during flame spread, but much more so during burnout (Fig. 2).

5. Model development

5.1. Vertical flame spread

Discrete flame spread for our configuration can be envisioned as a series of ignitions between many thermally-thin elements, following previous work by Gollner et al. [10]. The ignition time for a thermally thin material can be expressed as

$$t_{ig} \approx \rho_s c_{p,s} d(T_p - T_\infty)/\dot{q}'' \tag{1}$$

where t_{ig} is the ignition time (assuming t_{ig} is much longer than kinetic or transport effects), ρ_s, $c_{p,s}$, and d are the density, specific heat and diameter of the solid, T_p is the pyrolysis temperature, T_∞ is the ambient temperature, and $\dot{q}''$ is the net heat flux from the flame to the fuel surface, including heat losses. In Eq. (1) piloted ignition is assumed because observations show flames reside close to neighboring dowels (the maximum separation is only 1.5 cm) and the diameter rather than the radius of the dowel is used because, at the time of ignition, flames primarily reside only around the lower half of the dowel. Calculations show that, in horizontal spread, losses remain less than 10% of the total heat flux and less than 6% for vertical flame spread. Typically for a buoyant flow, the Grashof number would be used to represent convection. However, when the spacing S is sufficiently larger than the diameter, d, the upper cylinder will lie in the "far wake" of the lower cylinder, which should occur when S/d is greater than 2, the case for all spacings in this study [16]. By calculation we found that the Grashof number during wooden array burning is around $\mathrm{Gr} = 10^{5.9}$–$10^{6.3}$, which is very close to the assumption of $\mathrm{Gr} = 10^6$–10^9 in [16], showing that a "far wake" assumption is reasonable in this study.

Convective heat transfer to the cylinder surface can be described by a Nusselt number correlation, here taken from Albini and Reinhardt [17] which simplified the correlation from Marsters [16] and applied it to heating of wooden cylinder by a flame [17],

$$\mathrm{Nu} = 0.344\,\mathrm{Re}^{0.56}, \tag{2}$$

where

$$\mathrm{Re} = \rho_g u_g d/\mu_g, \tag{3}$$

and

$$\mathrm{Nu} = hd/k_g, \tag{4}$$

where Re is the Reynolds number. ρ_g, μ_g, and k_g are the density, viscosity, and conductivity of air, respectively and u_g is a buoyant velocity estimated by the height of the burning zone, $u_g = \sqrt{gx}$. This height above the first ignited cylinder, x can be calculated as,

$$x = (S + d)n + d, \tag{5}$$

where n is the rows number of the burning wooden dowels and S is the spacing between dowels. The burnout time also needs to be found in order to calculate the instantaneous height of the pyrolysis region when calculating mass-loss rates. The burnout time for a fuel cylinder can be expressed by [10]

$$t_b = \frac{\rho_s c_{p,g} d^2 \left[2\ln\left(2r_f/d\right) + 1\right]}{16 k_g \ln(1 + B)}, \tag{6}$$

where $c_{p,g}$ is the specific heat of the surrounding gas at $(T_f + T_p)/2$, r_f is the flame standoff radius taken from correlations, $\ln(2r_f/d) = 0.2(d/2)^{-0.75}$ with d in centimeters [18], and B is the fuel mass-transfer number, [10], which represents the burning properties of the fuel. This theoretical extension developed by Gollner et al. based on a constant burning rate assumption has been shown to match ignition and burnout of a single vertical column of wooden dowels well [10].

5.2. Horizontal flame spread

While vertical ignition and flame spread appear to be dominated by convection, inspection of experimental video reveals that flames do not contact dowels horizontally adjacent to one another, suggesting that radiation is the dominant mode in the horizontal direction. In order to evaluate the radiation received by a horizontal virgin dowel from a neighboring flame, a view factor from the flame to the target can be formulated from [19,20]. We suppose that the flame appears as a rectangle parallel to neighboring virgin dowels, which, by visual inspection of video footage, appears to be a reasonable assumption. If the center of the neighboring virgin dowel can be ignited by flame radiation, then the flame can spread horizontally. The view factor, F, of the flame to a parallel virgin dowel can be expressed as

$$F = \frac{1}{2\pi}\left\{\frac{l\arctan\left[2S\tan\theta\left(l^2/4 + S^2\right)^{0.5}/\left(S^2 + l^2/2\right)\right]}{\left(l^2/4 + S^2\right)^{0.5}} - 2\arctan\left(\frac{l\cos\theta}{2S}\right)\sin\theta\right\}, \tag{7}$$

where l is the length of wooden dowels and θ=arctan(H/S) is the angle made between the top of the flame H and an adjacent virgin dowel. As most of the flame resides below the top-most dowel, H is approximated as the height of the top-most ignited dowel, predicted by Eqs. (2–6). While this approximation neglects some of the flame height, it was found to have a negligible effect on the view factor (Eq. 7) when comparing measured flame heights in horizontal spread experiments to those estimated here, therefore it was neglected to simplify the analysis. The radiation received by a virgin dowel can then be expressed by

$$\dot{q}''_{rad} = F\sigma\varepsilon(T_f^4 - T_\infty^4), \tag{8}$$

where $\varepsilon = 1 - e^{-3.11L}$ is used to estimate the emissivity of the flame. This correlation, based on small-scale tests of fine forest fuels calculates emissivity as a function of height with L, here taken as the pyrolysis length (height of the burning region) [21,22]. While neighboring dowels may also contribute some heating due to re-radiation, estimates show that these contributions would be small for the spacings studied here ($< 1.27\,\mathrm{kW\,m^{-2}}$ for the 0.75 cm spacing and $0.76\,\mathrm{kW\,m^{-2}}$ for the 0.875 cm), therefore they are neglected. Combining Eqs. (1,7,8), the horizontal ignition time can be calculated. The input parameters used to estimate vertical and horizontal ignition times based on Eqs. (1–8) are presented in Table 1. Wood thermophysical properties were estimated at ambient conditions using average values for birch wood to make predictions possible a priori.

5.3. Mass-loss rate model

Emmons hypothesized that the shear stress over a burning fuel surface should be proportional to the mass burning rate at the surface [25]. Combining an extension of Reynolds analogy and Emmons hypothesis [26], the mass loss rate at the solid fuel surface can be expressed as,

$$\dot{m}''_f = \frac{Bk_w}{c_{p,s}L}\left(\frac{\partial T^*}{\partial y^*}\right)_{y^*=0} \tag{9}$$

where $Bk_w/c_{p,s}$ is a constant representing properties of the fuel and L is a characteristic length. $(\partial T^*/\partial y^*)_{y^*=0}$ is a non-dimensional temperature gradient normal to the cylindrical dowel surface. The Nusselt number is related to this quantity,

$$\mathrm{Nu} = \frac{hL}{k_w} = \left(\frac{\partial T^*}{\partial y^*}\right)_{y*=0}. \tag{10}$$

All properties are evaluated at a film temperature, $(T_f\text{-}T_p)/2$. L is a characteristic length related to the average height of the burning area derived from the ratio of burning area to the total area of the array, represented as

$$L = 2\left[N(a-1)^2S^2/a^2\pi\right]^{0.5}, \tag{11}$$

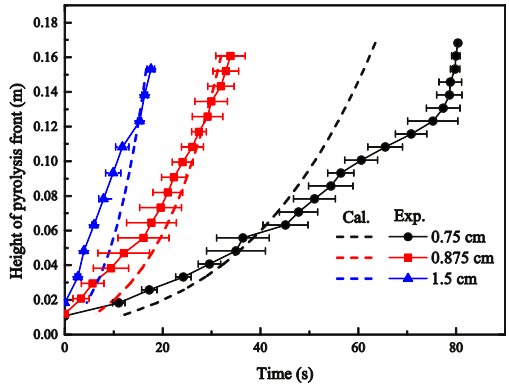

Fig. 3. The height of the pyrolysis front, defined as ignition of a dowel along the centerline as a function of time is compared to calculations (Cal.) using a convection-based theory (Eqs. 1–5).

where N is the number of burning wooden dowels at a particular moment in time, t, and a is the number of rows and columns of the whole wooden dowel array. The total number of burning dowels (N in Eq. 11) is computed at each time step using Eqs. (1–8). L can then be thought of as an instantaneous, average pyrolysis height, incorporating the fact that the spreading area may not be uniform across the width as the flame front evolves over time. The Nusselt number found in Eq. (2) can then be used to calculate the heat transfer to each dowel in Eqs. (9 and 10) as a function of time, incorporating the growing height of the burning region which increases the velocity of gases and therefore heating rates. By solving Eqs. (2,3,9–11) numerically, the global mass loss rate at any one time can then be calculated.

6. Results and discussion

6.1. Vertical flame spread

Figure 3 shows the advancement of pyrolysis front along the centerline as a function of time compared to the convection-based theory as a dashed line. This comparison is reasonable, especially when considering the ignition was distinguished visually from video. As expected, the flame spread rate increases as the spacing increases, which was found to occur due to increased buoyant velocities and thus increased convective heating with height [10]. It also appears that, as the 0.75 cm spacing spreads upward, it starts to deviate from theory, spreading slower. This is the densest array and even appears to have an oxygen-limited regime at later stages, so some of these features may not be captured by the simplistic 1-D theory. The influence of many dowels burning may also generate larger convective flows that are not incorporated in

a 1-D theory. While measurements of the ignition time were taken for all dowels in the array, only centerline results are presented for upward spread, as results follow the same trends in adjacent columns.

6.2. Horizontal flame spread

Using Eqs. (7 and 8), we can calculate the radiation received by adjacent virgin dowels as a means to estimate horizontal rates of flame spread. For the largest spacing, 1.5 cm, there is not enough radiation transmitted to ignite adjacent dowels before the first dowels burn out, therefore there is no horizontal flame spread. For $S = 0.75$ and 0.875 cm, radiation increases as a function of pyrolysis height, with more dowels burning as the flames spread upward, extending the length of the flame that heats adjacent dowels.

Prior to applying the horizontal flame spread model from Section 5.2 to the full arrays, some smaller horizontal flame spread experiments were performed. The same backing was used to test flame spread in the horizontal direction but the number of vertical rows was varied from 3 to 8 tall. Spacings of 0.875 and 0.75 cm were used. The above range of conditions was selected because these were where flames would actually spread horizontally. These experiments made it easier to observe the slower mode of horizontal flame spread and compare it with a radiation-based model without rapid vertical flame spread influencing results.

Figure 4 shows horizontal flame spread through these arrays with varying numbers of vertical rows with 0.75 and 0.875 cm spacings. Experimental ignition times were found using high-speed video, as previously described, and the radiation-based model was used to predict horizontal spread times. It can be seen in Fig. 4 that horizontal spread follows a linear trend at a nearly constant rate, indicating the assumption of a radiation-based model, which must result in steady rates of spread is reasonable. For all conditions, experimental flame spread data match the radiation based-theory calculations reasonably well, with an increasing horizontal flame spread rate with increasing flame radiation from additional vertical rows.

To investigate the horizontal spread model further, Fig. 5 shows a comparison of flame spread in the horizontal direction between experiments with full arrays and calculations with 0.75 and 0.875 cm spacing. There is variation observed between the ignition times as a function of the vertical row, as vertical convection must influence heating and cooling of the dowels, though its influence is small because the horizontal flame spread rate is generally constant. The predicted ignition times therefore predict horizontal flame spread through the arrays well within the experimental error.

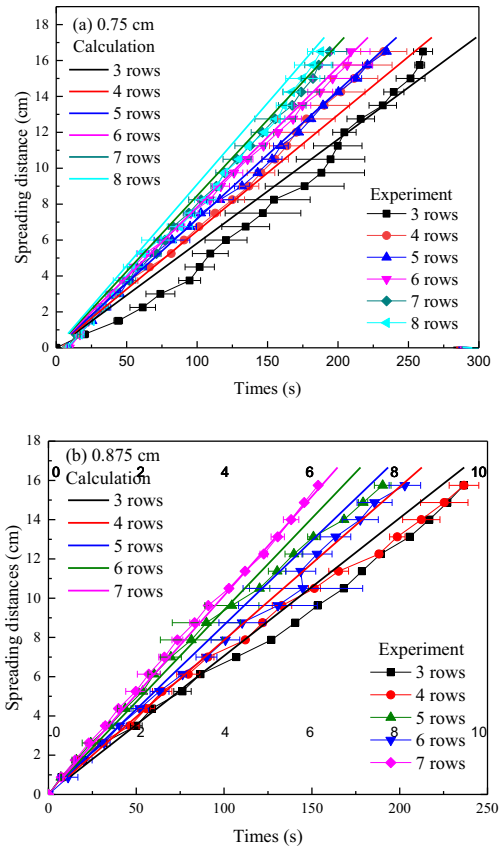

Fig. 4. Comparison of horizontal spread experiments and calculations for spread through an array 3–8 rows tall for 0.75 and 0.875 cm spacings.

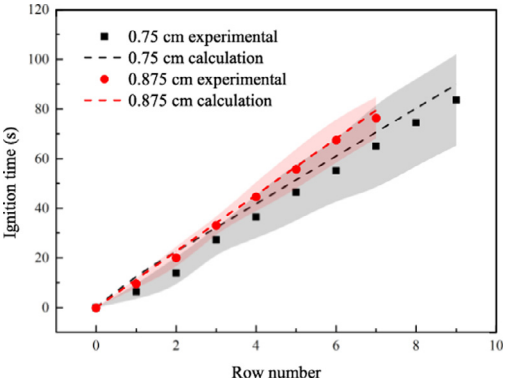

Fig. 5. Comparison of experimental and calculated horizontal flame spread for 0.75 and 0.875 cm spacings for full arrays of wooden dowels. The vertical axis indicates the ignition time of dowels following ignition of the first dowel. The shaded region indicates variations in experimental measurements, including the left and right halves of the arrays.

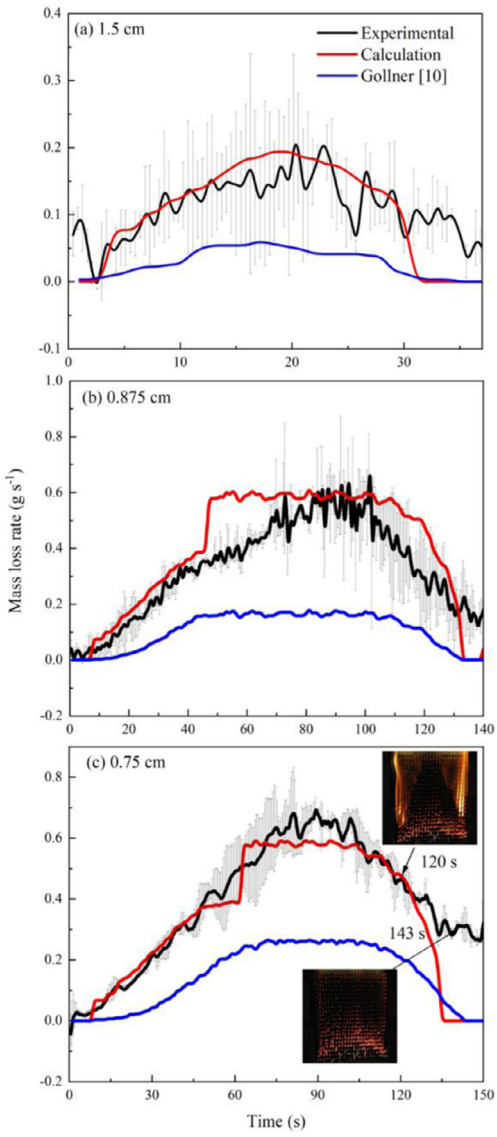

Fig. 6. Mass-loss rate comparisons of experimental data (black), calculated results in this study (red), and previous study (blue) with three spacings: (a) 1.5 cm; (b) 0.875 cm; (c) 0.75 cm.

6.3. Prediction of mass loss rate

Combining models for horizontal and vertical flame spread rates, the number of burning wooden dowels was calculated at each moment, N. In previous experiments on a single vertical row of wooden dowels, the total mass-loss rate was calculated based on the flame spread rate and an estimation of the steady mass-loss rate for a single wooden dowel [10]. However, this method works only for small arrays where the interaction between dowels is minimal. Using a new mass-loss rate model based on Emmons's hypothesis we are able to incorporate an average length of the burning region, L, Eq. (11), which varies based on the position and number of dowels burning at any one time. This serves to incorporate some influence of the surrounding dowels, though it will neglect some effects such as fuel-rich conditions at the center of the array and smoldering after flames are extinguished.

Using Eqs. (9–11), the theoretical variation of mass-loss rate can be obtained. Collected mass loss data from the load cell was smoothed and a finite-difference scheme applied to calculate the mass-loss rate. Figure 6a shows this data compared with calculated results from this study as well as comparison to a previous model used by Gollner et al. [10]. For $S = 1.5$ cm, only one column of dowels ignites, and the calculated mass-loss rate matches the experimental mass-loss rates relatively well, especially during the first 20 s as new dowels are ignited. As sticks burn out the calculation deviates a bit, but this may be more due to the burnout theory which is the same as used by Gollner et al. [10]. The "spikey" nature of the mass-loss rate, due to each dowel igniting, is not captured by the model, however the calculated mass-loss rate follows the same averaged trend very well.

For the 0.75 and 0.875 cm spacings, the flames spread both vertically and horizontally, as shown in Fig. 2. The vertical flame spread velocity is much faster than in the horizontal direction, which results in an interesting phenomenon where the central column burns out while leaving some dowels burning and spreading towards the sides. The burning area then breaks up into two plumes that spread from the center of the array to the side. So, from the moment that a burnout area develops in the center, the convection column becomes separated into two parts, so the characteristic length scale for the convective heat transfer calculation (Eq. 11) is modified and the calculation is split into two separate left and right burning areas. Results are compared for the 0.75 and 0.875 cm spacings shown in Fig. 6b and c. At around 53 s, this separation of the flame front happens in both cases (a sharp rise in the red calculated line). Again, the mass-loss rate observed in the initial stage before the separation of the flame fronts fit very well with the model. It appears both the individual burning rates of wooden dowels and the initial spread is well-modeled. The assumption that burning stops completely is not entirely accurate, as wooden dowels actually smolder and have a small amount of mass loss which decays over time, starting to introduce errors as a larger array of sticks is burning out. From the image of the burned-out array in Fig. 6c, we can find that although the flame has extinguished at 143 s, the wooden array still had some obvious mass loss, which was caused by smoldering of remaining char.

7. Conclusions

In this study, a series of wooden dowel arrays with different spacings, 1.5, 0.875, and 0.75 cm, were burned to explore the mechanisms of flame spread between arrays of discrete fuels. For the largest spacing, 1.5 cm, flames would spread only vertically along the central column, there was no horizontal spread towards both sides. For the smaller 0.75 and 0.875 cm spacings, flames would spread both vertically and horizontally simultaneously. The vertical flame spread rate was much faster than that in the horizontal direction. Even after the central columns burned out, flames would continue to spread horizontally. Based on these experiments, two new models were developed. A radiation-controlled model was used to predict the horizontal flame spread rate and Emmons hypothesis was used to develop a theory for the mass-loss rate of a burning dowel which incorporated effects of surrounding flames through a length scale parameter. Using an existing theory for vertical flame spread based on convection heat transfer, flame spread through the 2-D array was predicted. Using these predictions, the mass-loss rate was also predicted. The use of simple models such as these are well suited to large arrays where assumption of a homogenous fuel is not well modeled by existing techniques and could be too computationally intensive for a full, multi-physics numerical simulation.

Acknowledgments

JS and LJ were supported by the National Key Research and Development Plan (No. 2016YFC0800100) and the National Natural Science Foundation of China (NSFC, Grant 51806208). Support for WT, CM and MG came from the National Science Foundation under Grant No. CBET-1554026.

References

[1] M.J. Gollner, X. Huang, J. Cobian, et al., *Proc. Combust. Inst.* 34 (2) (2013) 2531–2538.
[2] L. Jiang, C.H. Miller, M.J. Gollner, J.H. Sun, *Proc. Combust. Inst.* 36 (2) (2017) 2987–2994.
[3] L. Jiang, J.J. He, J.H. Sun, *J. Hazard. Mater.* 342 (2018) 114–120.
[4] A.C. Fernandez-Pello, T. Hirano, *Combust. Sci. Technol.* 32 (1983) 1–31.
[5] F.A. Williams, *Prog. Energy Combust.* 8 (4) (1982) 317–354.
[6] K. Takeno, T. Hirano, *Proc. Combust. Inst.* 21 (1) (1988) 75–81.
[7] I.T. Leventon, J. Li, S.I. Stoliarov, *Combust. Flame* 162 (10) (2015) 3884–3895.
[8] J.W. Kwon, N.A. Dembsey, C.W. Lautenberger, *Fire Technol.* 43 (4) (2007) 255–284.
[9] M. Vogel, F.A. Williams, *Combust. Sci. Technol.* 1 (6) (1970) 429–436.
[10] M.J. Gollner, Y. Xie, M. Lee, et al., *Combust. Sci. Technol.* 184 (5) (2012) 585–607.
[11] M. Finney, D. Jack, M. Jason, et al., *Proc. Natl. Acad. Sci.* 112 (32) (2015) 9833–9838.
[12] G.F. Carrier, F.E. Fendell, M.F. Wolff, *Combust. Sci. Technol.* 75 (1991) 31–35.
[13] M.F. Wolff, G.F. Carrier, F.E. Fendell, *Combust. Sci. Technol.* 77 (1991) 261–289.
[14] H.W. Emmons, T. Shen, *Proc. Combust. Inst.* 13 (1) (1971) 917–926.
[15] J.M. Prahl, J.S. Tien, *Combust. Sci. Technol.* 7 (1973) 271–282.
[16] G.F. Marsters, *Int. J. Heat Mass Tranf.* 15 (5) (1972) 921–933.
[17] F.A. Albini, E.D. Reinhardt, *Int. J. Wildland Fire* 5 (2) (1995) 81–91.
[18] C.K. Lee, *Combust. Flame* 32 (1978) 271–276.
[19] J.L. Rossi, A. Simenoni, B. Moretti, L. Leroy-Cancellieri, *Fire Saf. J.* 46 (8) (2011) 520–527.
[20] L. Zarate, J. Arnaldos, J. Casal, *Fire Saf. J.* 43 (8) (2008) 565–575.
[21] E. Pastor, A. Rigueiro, L. Zarate, et al., *Wildland Fire Saf. Summit* (2002) 1–11.
[22] D.L. Simms, M. Law, *Combust. Flame* 11 (5) (1967) 377–388.
[23] T.L. Bergman, F.P. Incropera, A.S. Lavine, *Fundamentals of Heat and Mass Transfer*, John Wiley & Sons, 2011.
[24] K. Annamalai, M. Sibulkin, *Combust. Sci. Technol.* 19 (5–6) (1979) 167–183.
[25] H.W. Emmons, Z. Angew, *Math. Mech.* 36 (1956) 60–71.
[26] A.V. Singh, M.J. Gollner, *Proc. Combust. Inst.* 36 (2) (2017) 3157–3165.